GEOLOGICA BALCANICA 51 (1), Sofia, April 2022, pp. 3–14.

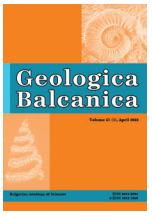

The discovery of U mineralization in the late Variscan plagiogranite vein of the Shkhara crystalline massif (Greater Caucasus, Georgia)

Avtandil Okrostsvaridze[1], *David Bluashvili*[2], *Salome Gogoladze*[1], *Rabi Gabrielashvili*[2]

[1] *Institute of Earth Sciences, Ilia State University, 77 Ntsubidze Str., 0177 Tbilisi, Georgia; e-mails: okrostsvari@gmail.com (corresponding author), salome.gogoladze.2@iliauni.edu.ge*
[2] *Faculty of Mining and Geology, Georgian Technical University, Kostava Str., 0175 Tbilisi, Georgia; e-mails: datoblu@yahoo.com, rabi.gabrielashvili.1@iliauni.edu.ge*

(Received: 03 January 2022; accepted in revised form: 28 February 2022)

Abstract. The Greater Caucasus belt is the northernmost expression of the Caucasus orogen and is linked to the southern margin of the Precambrian Scythian Platform. In the pre-Jurassic crystalline basement of this belt, a plagiogranite vein, exposed in the headwaters of the Enguri River, with elevated radiation (μSv/h range of ~1–3), has been discovered. The vein is located along the Main Thrust of the Greater Caucasus, in the upper Paleozoic biotite migmatites of the Shkhara crystalline massif. It is ~2–3 m thick and represents hydrothermally altered rock (SiO_2 content varies from ~75% to ~85%) predominantly composed of a quartz-plagioclase assemblage. LA-ICP-MS $^{206}Pb/^{238}U$ dating of zircons from the vein indicates an age of 310.2±7.5 Ma that corresponds to the late Variscan orogenic activity. The vein is slightly fragmented and fractured, and fractures and nests are filled with Th-enriched uraninite veins and impregnations. According to ICP-MS-ES analyses, the Th content varies from ~26 ppm to ~50 ppm, and the U varies between ~55 ppm and ~290 ppm. Based on the conducted research, it was found that there is a full correlation between the studied vein and U-bearing granitic veins of different regions of the world by composition, magma series, geodynamic setting, tectonic location and isotopic age. On this basis, it is supposed that the late Variscan hydrothermally altered plagiogranite veins, which are localized in the shear zones of the Shkhara Massif, and entirely in the Main Range Zone of the Greater Caucasus, are potentially U-bearing.

Okrostsvaridze, A., Bluashvili, D., Gogoladze, S., Gabrielashvili, R. 2022. The discovery of U mineralization in the late Variscan plagiogranite vein of the Shkhara crystalline Massif (Greater Caucasus, Georgia). *Geologica Balcanica* 51 (1), 3–14.

Keywords: Greater Caucasus, Shkhara Massif, plagiogranite vein, uraninite.

INTRODUCTION

It is a well-known fact that thick felsic melts that formed in subduction zones and experienced post-magmatic hydrothermal activity in the upper part of these structures are often enriched in economic deposits of metals (*e.g.*, Groves and Bierlein, 2007; Ridley, 2013; Richards, 2015; Zheng *et al.*, 2019). These types of geodynamic regimes also form hydrothermal vein-type uranium deposits, which make up ~30% of the global uranium reserves. Two main types of these uranium ore deposits are distinguished: granitic vein-like and breccia complex (*e.g.*, Rene, 2012). Breccia complex-type uranium ore deposits are mostly related to Proterozoic rocks (Ukraine, Australia, Africa), whereas vein-type ones are related to Upper Paleozoic and Mesozoic granitoids (Spain, France, Germany, Namibia,

https://doi.org/10.52321/GeolBalc.51.1.3

south China) (*e.g.*, Basson and Greenway, 2004; Bonnetti *et al.,* 2018). Uranium concentration in the vein-type deposits is typically within ~200 ppm and, as a rule, their formation is associated with the late orogenic activities of magmatism (*e.g.*, René, 2012; Ballouard *et al.*, 2017).

The dominant part of the uranium deposits in granites is associated with the Late Carboniferous peraluminous veins of the Variscan orogeny. These veins are localized in brecciated or fault zones that may occur in both the center and peripheries of granitic massifs. In Europe, those types of uranium deposits have been identified in the Iberian Massif, Spain (*e.g.*, López-Moro *et al*., 2019); in the Armorican and Central Massifs, France (Cuney, 2014); in the Schwarzwald Massif, Germany (Hofmann and Eikenberg, 1991); and in the Bohemian Massif, the Czech Republic (*e.g.*, Dolníček *et al*., 2013). In Canada, the important uranium vein-type deposits of late orogenic activity are associated with Proterozoic granites (northern Saskatchewan) (*e.g.*, Chiu *et al.*, 2020), while in Namibia (Damara orogeny) and southern China (Yanshanian orogeny) the uranium vein deposits are associated with Jurassic granites (*e.g.*, Basson and Greenway, 2004; Zhang *et al*., 2017).

In 2020, high concentrations of thorium and uranium were discovered during field investigations in one of the plagiogranite veins of the Shkhara Massif. This paper considers the primary information of research on this vein, which will enrich the general knowledge on the uranium and thorium hydrothermal mineralizations. We believe that the results of this study can be used in further prospection for new uranium and thorium ore occurrences in the Greater Caucasus, as the demand for these elements will increase sharply in the future (see Van Gosen *et al*., 2009; Tulsidas *et al*., 2015; Ault *et al*., 2016).

GEOLOGICAL BACKGROUND OF THE REGION

The Caucasus orogenic belt extends in a NW–SE direction from the Caspian Sea to the Black Sea, at a distance of more than 1200 km. This belt resulted from the successive collisions and accretions of the Gondwana-derived Rhodope-Pontides, Anatolia and Arabia crustal blocks to the Scythian Platform of the Eurasian continent during the closure of the Paleo-Tethys and Neo-Tethys oceans since the Paleozoic (Şengör and Yılmaz, 1981; Gamkrelidze, 1986; Stampfli and Borel, 2004; Okrostsvaridze and Tormey, 2013).

The Greater Caucasus fold-and-thrust belt is the northernmost expression of the Caucasus orogen and is linked to the southern margin of the Precambrian Scythian Platform. In the structure of the Greater Caucasus, two major formations are distinguished: pre-Jurassic crystalline basement and Meso-Cenozoic magmatic and sedimentary formations. It has been opined that the pre-Jurassic basement in the Paleozoic was an active continental margin, along which Paleo-Tethys oceanic crust was subducted to the north (Gamkrelidze, 1986; Gamkrelidze and Shengelia, 2005; Okrostsvaridze, 2007; Okrostsvaridze and Tormaey, 2011).

The basement complex of the Greater Caucasus has a collage construction, which is thrust upon the Lower Jurassic formations along the Main Thrust of the Greater Caucasus (MTGC). In general, within the basement complex, four regional structural-tectonic zones are recognized from south to north: Southern Slope, Main Range, Fore Range and Bechasyn (Somin, 2011; Gamkrelidze *et al.*, 2020).

The Main Range Zone is the best-exposed part of the basement complex. Because of differences in the structure and composition, it is divided into two subzones: the Pass (to the South) and the Elbrus (to the North). These subzones are in tectonic contact along the Alibak-Urukh regional fault. The Elbrus Subzone is dominantly built up by sialic rocks, which have undergone LP-HT type of metamorphism. In contrast, the Pass Subzone contains mostly felsic rocks, but it has also been subjected to LP-HT type of metamorphism (Gamkrelidze and Shengelia, 2005).

In the crystalline basement of the Greater Caucasus, the Variscan plutons are localized in both the Pass and Elbrus subzones of the Main Range Zone. In the Pass Subzone, the plutons are mainly represented by I-type quartz-diorites and granodiorites, while the Elbrus Subzone is characterized by S-type two-mica granites. In both subzones, these plutons cut through the Upper Paleozoic gneiss-migmatite infrastructure. It is noteworthy that, in the infrastructure, as well as in the intersected plutons, ~0.3–4.5 m thick plagiogranite veins are developed. These veins are not usually affected by the regional microclinization, which is one of the main pieces of evidence that they are late orogenic formations (Okrostsvaridze, 2007).

The Greater Caucasus is rich in gold, tungsten, antimony and other deposits (*e.g.*, Okrostsvaridze and Bluashvili, 2009; Okrostsvaridze *et al*., 2014, 2016); however, neither uranium nor thorium ore mineralisations have been discovered to date (see Okrostsvaridze and Gogoladze, 2017). In this re-

gion, exploration activities were carried out to search for uranium and thorium during the Soviet period, about which there is no information available. The only publication concerning the geology of uranium and thorium is that of Odikadze (1971). In the latter paper, uranium and thorium geology was discussed, based on geochemical analyses of samples of granitoids from the Greater Caucasus and the Dzirula Massif, but high concentrations of uranium and thorium were not detected. Odikadze (1971) concluded that the average contents of these elements correspond to 9 g/t and 14 g/t, respectively. Also, this author pointed to the fact that, in the late Hercynian granites of the Caucasus, the uranium content is three to five times higher than its average concentration in Earth's crust, which indicates the uranium geochemical specialization of these rocks. Our investigation confirms this statement.

Shkhara Massif

The Shkhara crystalline massif is located at the headwaters of the Enguri and Khalde rivers, in the Svaneti historical province. The province is located in the central, highest, elevation portion of the Greater Caucasus and covers more than 7,000 km^2 area. The crystalline basement is overlain by Mesozoic sedimentary deposits and intersecting plutons (Fig. 1). The Shkhara Massif builds a ~15 km long and ~5 km high beautiful ridge (Fig. 2). It is composed of Lower to mid-Paleozoic biotite schists, gneisses and migmatites (gneiss-migmatite complex), cut by a huge granitoid pluton of the Variscan orogeny generation. It is in active tectonic contact with the Lower Jurassic mudrocks and is thrust over these rocks to the south. The Shkhara pluton is interpreted as a formation of mantle-crustal generation, which formed under the geodynamic setting of an island arc. It is predominantly composed of granodiorites, with lesser amount of granites and quartz-diorites. The SiO_2 content in the granodiorites varies between ~67% and 71%, with Al_2O_3 content of ~14% to 16%; Fe_2O_3 content of ~3–6 %; MgO content of ~0.5% to 1%; Na_2O content of ~2.5% to 3.5 %; and K_2O content of ~3% to 4% (Okrostsvaridze, 1995). The Shkhara Massif is characterized by numerous enclaves of biotite-migmatites and gneisses, the volumes of which may reach several cubic meters. Since the entire complex experienced intense microclinization, microcline granites formed in some areas. Zircons in granodiorites of the main phase of the Shkhara pluton and enclosing biotite-gneisses

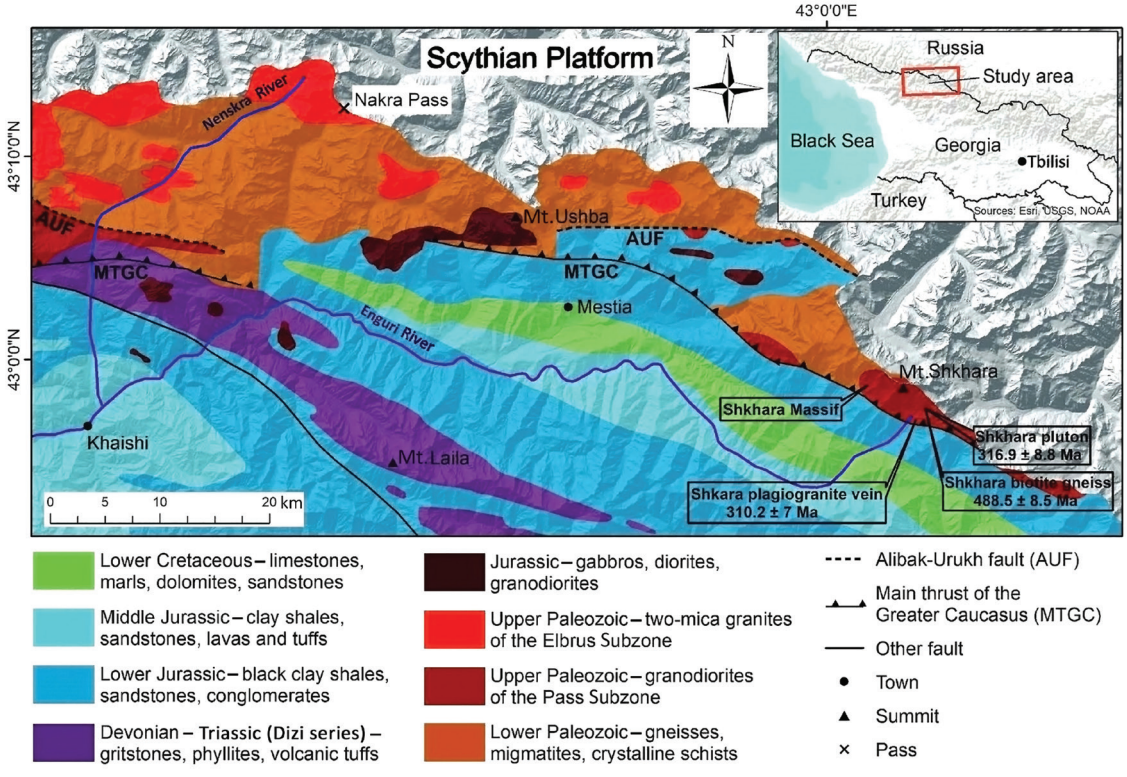

Fig. 1. Simplified geological map of the headwaters of the Enguri River, with zircon U-Pb geochronological data on the Shkhara Massif (Greater Caucasus, Georgia).

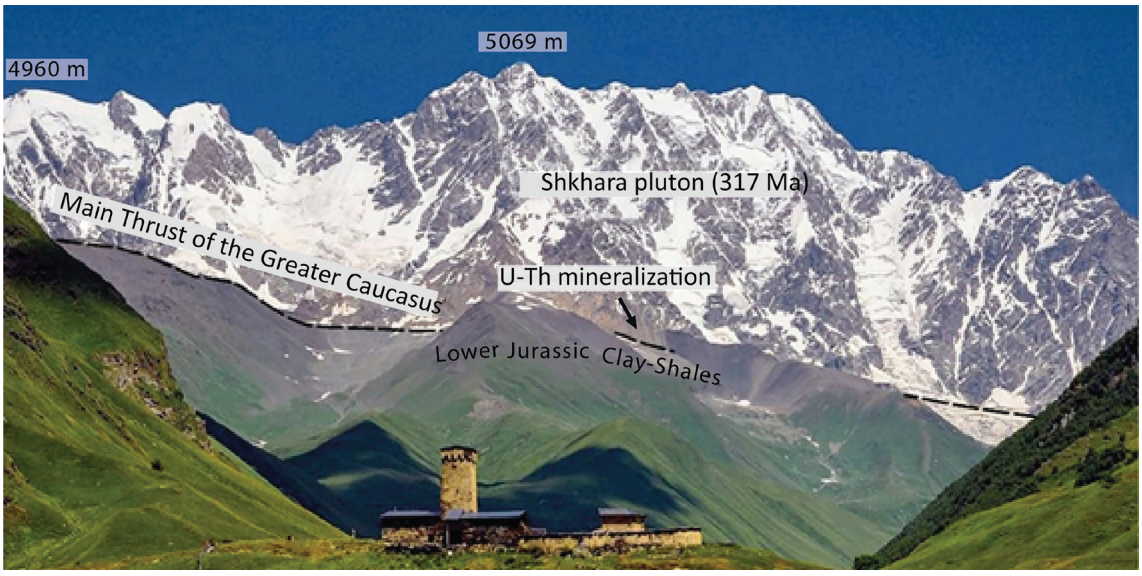

Fig. 2. Exposed parts of the Shkhara Massif, viewed from the south. In the foreground are the Svanian tower and the medieval Georgian Orthodox church.

were dated by the LA-ICP-MS method. This study found a weighted mean $^{206}Pb/^{238}U$ age of 316.9± 8.8 Ma for zircons of the Shkhara pluton granodiorites, compared to a weighted mean $^{206}Pb/^{238}U$ age of 488.5±8.5 Ma for zircons of the biotite gneiss (unpublished data).

Plagiogranite veins of different thicknesses (~0.5–4 m) often cut the Shkhara Massif. They occur along the Main Thrust and mark the Paleozoic suture zone. From the east to the west of this thrust, the veins are exposed to the southern edges of the Kamenistaia, Beshta, Saken, Szgimazuk and Shkhara massifs. In terms of petrochemical, isotopic and thermobaric parameters, these massifs are interpreted as partial melting products of subducting oceanic crust, or re-melting of accreted oceanic crust (Okrostsvaridze, 1995). Apart from these plagiogranites, anatectic plagiogneisses and plagiogranites also occur in the gneiss-migmatite infrastructure of the Greater Caucasus crystalline basement. The latter are located in the shape of coherent bodies in the containing rocks. It is noteworthy that, during an expedition in 2021, the elevated radiation dose (μSv/h > 1) was detected in several anatectic plagiomigmatite boulders (~2 m by 3 m). A radioactive hydrothermal plagiogranite vein was discovered in the central segment contact area of the Shkhara Massif. It is located in a biotite migmatite along of the Main Thrust zone of the Greater Caucasus, in the headwaters of the Enguri River (42°58′45″N; 43°30′27″E). The vein has a thickness of ~2–3 m, dipping ~55° to 60° to the north, and extending in a NW–SE direction. Analogical high radiation vein was also discovered at the western periphery of the massif, in the headwaters of the Khalde River.

MATERIALS AND METHODS

During the field investigation, we studied the background radiation of the Shkhara plagiogranite vein using the FAG-FH40F2 dose rate meter. We took 12 samples for chemical analyses of the vein and its surrounding migmatites, each sample with an average weight of 2–3 kg. The whole-rock chemical compositions of these samples were measured using the different spectrometers in different laboratories: *1*) X-ray fluorescence spectrometer (XRF 2000) at the Geological Institute, Georgia (sample Nos. 20Sv1–20Sv12); *2*) ICP-MS analyses for 51 elements conducted by a laboratory contracted by the U.S. Geological Survey (USGS) (sample Nos. 20Sv1–20Sv5); and *3*) ICP-ES analyses for 48 elements conducted by MS – Analytical laboratory (MSALABS), Canada (sample Nos. 20Sv6–20Sv12).

One sample (21Geo-11), weighing ~5 kg, was taken from the Shkhara Massif plagiogranite vein for U-Pb zircon geochronology. A total of 25 zircon grains were separated and dated from this vein. The U-Pb zircon age determination analyses were conducted at the Department of Earth and Environ-

mental Sciences, National Chung-Cheng University, Taiwan, via laser ablation inductively coupled plasma mass spectrometry (LA-ICP-MS) equipped with an Agilent 7500s quadrupole and a New Wave UP213 laser ablation system. Calibration was performed using the GJ-1 zircon standard (Jackson *et al.*, 2004) and Plešovice zircon (Slama *et al.*, 2008) to assess data quality. All U-Th-Pb isotope ratios were calculated using GLITTER 4.4.2 (GEMOC) software, and the isotope ratio of common lead was corrected using the approach proposed by Andersen (2002). Isoplot v. 3.0 (Ludwig, 2003) was used to calculate weighted mean U-Pb ages and probability density curves. The detailed analytical procedure has been described by Chiu *et al*. (2009).

RESULTS AND DISCUSSION

Radiation dose of the plagiogranite vein

The radiation dose of the plagiogranite vein of the Shkhara Massif was measured in the field, using a FAG-FH40F2 dosimeter. The gamma radiation was measured in micro Sievert (μSv), which is a derived unit of ionizing radiation dose in the International System of Units (SI). This parameter is rated as a Sievert/hour. According to this parameter, the normal safe radiation dose for human health is ~0.17 in μSv/h (see ICRP Recommendations, 2007; Tulsides *et al.*, 2015).

The radiation dose varies from 1.5 μSv/h up to 2.0 μSv/h on the surface of the Shkhara plagiogranite vein (Fig. 3). In some places along the vein, this parameter increases to 2.7–3.0 μSv/h, but in some areas the radiation decreases from 1.2 μSv/h to 1 μSv/h. These values are almost 10–15 times higher than natural radiation. For this reason, we took eight samples from the vein for more detailed analyses. Moreover, we took four samples from the country rock adjacent to the vein, because here the background radiation is two times higher than the normal value (μSv/h > 0.30).

Fig. 3. Fragment of the Shkhara plagiogranite vein with FAG-FH40F2 dosimeter showing the radiation dose 2.06 μSv/h.

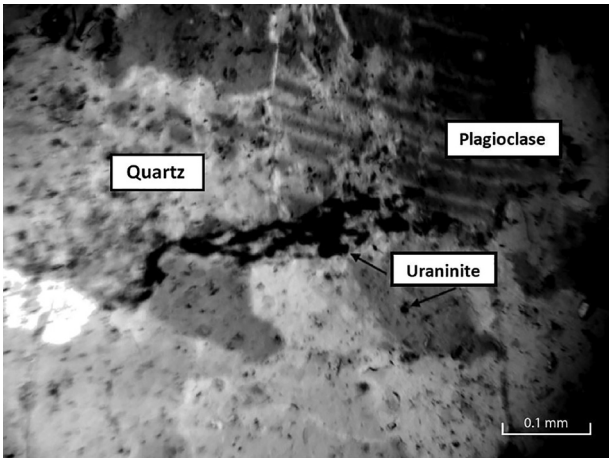

Fig. 4. Typical mineralogy of the uraninite vein and impregnations in plagiogranite of the Shkhara Massif; sample 21Sv8 (plane polarized light).

Petrography and geochemistry of the plagiogranite vein

The plagiogranite vein has a milky color, massive structure and medium to fine-grained texture. It is localized in biotite-migmatites and gneisses, which, unlike other rocks of the Shkhara Massif, have not undergone regional microclinization. The vein is mainly composed of quartz and plagioclase, with microcline, biotite, muscovite, chlorite and epidote present in minor amounts. Accessory minerals are allanite, zircon and sphene. The vein is slightly fractured and the cracks are filled with quartz. Intensive albitization and quartzitization were also observed and, in some places, the vein is completely quartzitized. Thorium-enriched uraninite occurs as impregnations in quartz-plagioclase masses (Fig. 4).

According to the geochemical study, the Shkhara plagiogranite vein is a felsic formation, in which SiO_2 content varies from 74.72% to 84.31%. The

Table 1
X-ray fluorescence (XRF) analyses of major elements and selected trace elements of the Shkhara Massif plagiogranite vein and containing migmatites

Sample	20Sv1	20Sv2	20Sv3	20Sv4	20Sv5	20Sv6	20Sv7	20Sv8	20Sv9	20Sv10	20Sv11	20Sv12
Major elements (wt. %)												
SiO_2	71.27	71.57	77.81	74.72	78.67	79.61	84.31	78.89	77.23	81.46	70.36	71.37
Al_2O_3	16.17	17.12	11. 13	11.5	10.58	11.5	10.09	10.94	11.34	10.05	15.3	16.22
Fe_2O_3	2.45	3.52	2.67	3.60	2.32	1.19.	1.02	3.17	2.81	1.17	2.28	2.46
CaO	1.77	2.08	1.52	3.62	1.31	1.48	1.39	1.85	1.66	1.36	1.54	2.36
MgO	0.56	0.89	0.98	0.84	0.83	0.57	0.17	0.25	0.57	0.54	0.81	0.64
Na_2O	3.90	3.86	3.34	3.18	3.86	3.86	3.40	3.92	3.88	4.03	2.53	2.15
K_2O	2.92	2. 92	1.57	1.65	1.25	1.73	1.52	1.34	1.57	1.27	2.58	3.14
MnO	1.07	0.87	0.33	0.27	0.21	0.12	0.03	0.13	0.28	0.37	1.12	0.46
TiO_2	0.7	0.6	0.58	0.45	0.28	0.18	0.15	0.19	0.32	0.14	0.87	0.43
P_2O_5	0.8	0.8	0.07	0.13	0.16	0.23	0.03	0.14	0.09	0.15	0.6	0.7
Trace elements (ppm)												
Rb	61.3	110	185.2.	114.2	279.8	334.7	185	134.5	318.4	175.6	58.2	64.7
Ta	0.38	0.72	1.28	1.59	0.95	2.04	1.28	1.59	1.45	1.89	0.27	0.65
Hf	0.2	0.4	0.1	0.1	0.4	0.1	0.3	0.3	0.1	0.1	0.6	0.3
Th	3.5	19,5	26.5	40.5	37.5	40.6	29.4	50.1	37.7	47.5	3.1	1.7
U	0.5	1.5	121	273	183	54.7	105.6	290.9	174	62.4	0.7	1.3
Nb	4.4	8.5	14.4	17.5	8.0	44.4	15.5	8.1	34.1	19.5	3.5	1.8
Tl	1.20	0.69	1.2	0.7	0.5	3.2	1.1	0.67	0.41	2.77	0.32	0.1
V	262	12	26	37	9	120	32	37	13	124	42	17
W	0.3	2.6	<1	<1	<1	2	0.4	0.4	0.3	2.1	0.7	0.3
Y	16.9	19.2	15.0	10.3	7.9	5.0	13.7	11.3	8.9	9.5	14.9	17.5

Samples: 20Sv1, 20Sv2, 20Sv11 and 20Sv12 – from migmatites; Samples: 20Sv3–20Sv10 – from plagiogranite vein.

other main elements are represented as follows: Al_2O_3 (10.05–11.34%); Fe_2O_3 (1.17–3.60%); MgO (0.17–0.98%); Na_2O (3.18–4.03%); and K_2O (1.25–1.73%) (see Table 1).

On the TAS classification diagram, all samples of the Shkhara plagiogranite vein are plotted within the granite field, but containing migmatites, also in the granodiorite field (Fig. 5*a*). On the AFM discrimination diagram, both plagiogranites and migmatites are plotted within the field of calc-alkaline magma series (Fig. 5*b*). On the Rb–(Nb+Y) geodynamic discrimination diagram, these rocks are plotted within both the volcanic arc granite and syn-collision granite fields (Fig. 5*c*), while on the Rb/30–Hf–Ta*3 discrimination diagram, only in syn-collision granite field (Fig. 5*d*).

Trace elements of the samples from the Shkhara plagiogranite vein show usual concentrations, but thorium and uranium contents are anomalously high. In four samples from the host rocks, U and Th contents vary from 1.7 ppm to 19.5 ppm and from 0.5 ppm to 1.3 ppm, respectively (see Table 1). These values are typical for unaltered gneisses. The concentrations of these radioactive elements drastically increase in the plagiogranite vein, which is displayed in Fig. 6.

In eight samples taken from this plagiogranite vein, Th contents vary in the range of 26.5 ppm to 50.1 ppm, whereas the U content ranges from 54.7 ppm to 290.9 ppm. As it can be seen from Fig. 6, the Th content in the vein is 7 to 10 times higher than the average crustal concentration, and the U content is 100 to 290 times higher. From these data, the U mineralization deserves special interest, since for granite veins of this type and age, as mentioned above, deposits with these U contents have been mined elsewhere (*e.g.*, Basson and Greenway, 2002; Descriptive Uranium Deposit, 2020).

Isotopic geochronology of the plagiogranite vein

One sample (21Geo-11) from the U-Th bearing plagiogranite vein was taken for the dating of zircons, using the U-Pb method (Table 2). It is a medium-grained, massive quartz-plagiogranite rock with the following mineral composition: quartz + plagioclase + microcline + biotite + muscovite + chlorite + allanite + zircon. We separated and dated 25 zircon grains from this sample. The grains represent small (~120×~60 μm) crystals, in which two zones can be

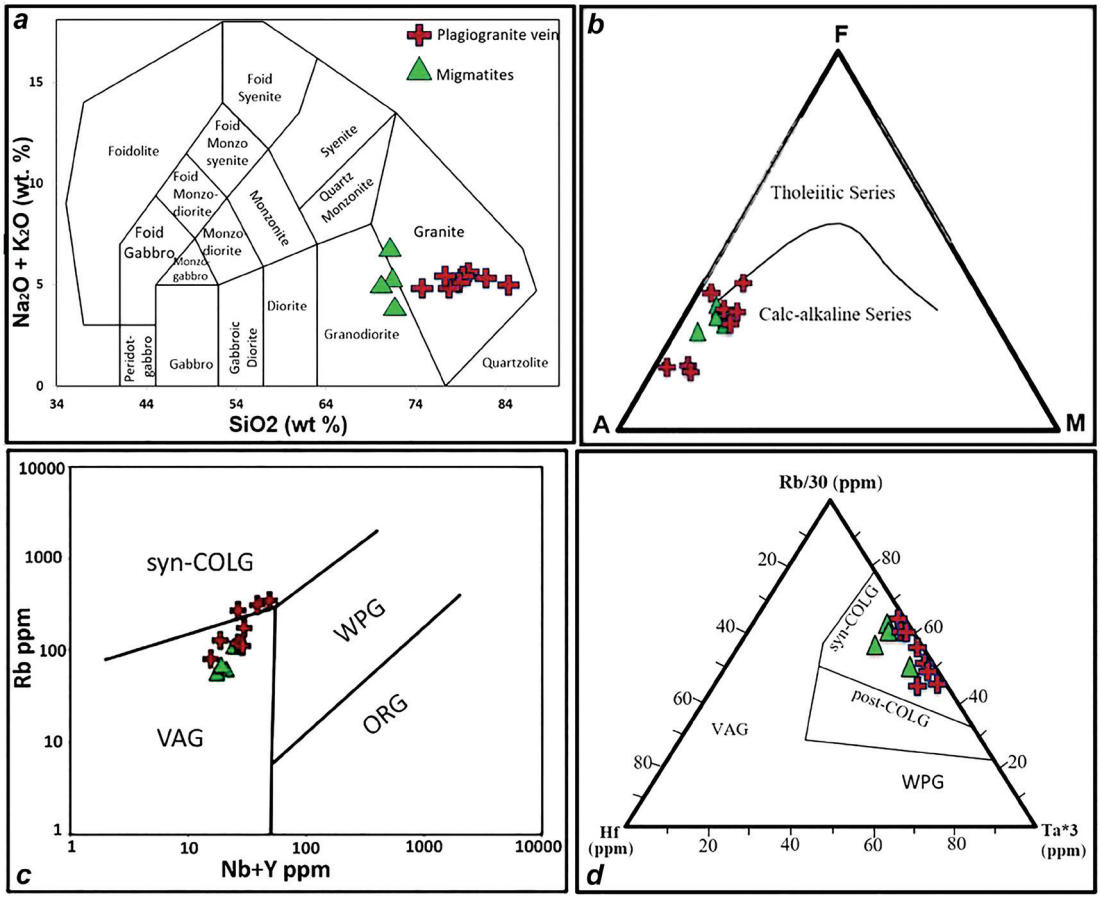

Fig. 5. Petrochemical diagrams for the plagiogranite vein and containing migmatites of the Shkhara Massif: *a*) TAS discrimination diagram (Middlemost, 1994); *b*) AFM discrimination diagram (Irvine and Baragar, 1971) (A = Na_2O+K_2O wt. %; F=FeO total wt. %; M=MgO wt. %); *c*) Rb–(Nb+Y) geodynamic discrimination diagram (Pearce, 1996); *d*) Rb/30–Hf–Ta*3 geodynamic discrimination diagram (Harris *et al.*, 1986). Abbreviations: syn-COLG = syn-collision granite; post-COLG = post-collision granite; VAG = volcanic arc granite; WPG = within-plate granite; ORG = ocean ridge granite.

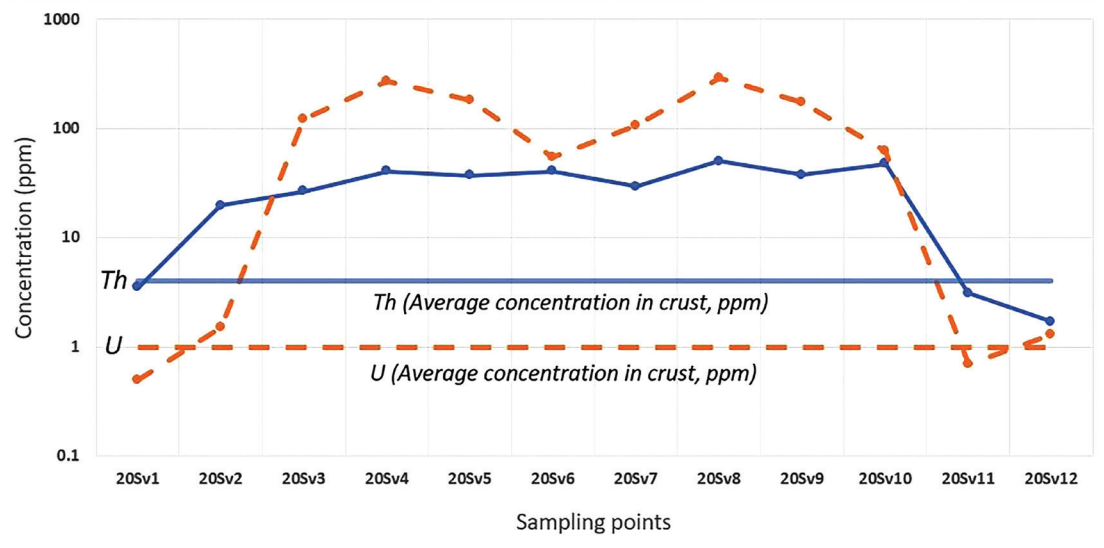

Fig. 6. Variation diagram of U and Th contents (ppm) in the plagiogranite vein of the Shkhara Massif (samples 20Sv3–Sv10) and containing migmatites (samples: 20Sv1; 20Sv2; 20Sv11; and 20Sv12).

Table 2
Zircon U-Th chemical analyses, U-Pb ratios and $^{206}Pb/^{238}U$ weighted mean ages of the Shkhara Massif plagiogranite vein (21Geo-11)

Spot	Th/U	U (ppm)	$^{207}Pb/^{206}Pb$	$^{207}Pb/^{235}U$	$^{206}Pb/^{238}U$	Error corr.	$^{206}Pb/^{238}U$ age (Ma)
1	0.41	309	0.0525	0.3529	0.0487	0.8728	308
2	0.33	369	0.0567	0.5461	0.0699	0.8851	432
3	0.53	602	0.0560	0.5407	0.0700	0.9292	435
4	0.17	450	0.0560	0.5029	0.0651	0.9103	407
5	0.55	293	0.0558	0.5351	0.0695	0.8744	432
6	0.93	137	0.0522	0.3396	0.0472	0.7526	297
7	0.47	134	0.0545	0.3643	0.0485	0.7656	305
8	0.20	278	0.0581	0.6087	0.0759	0.8849	472
9	0.01	1079	0.0535	0.3651	0.0495	0.8302	311
10	0.14	525	0.0543	0.4193	0.0561	0.8537	352
11	0.73	101	0.0530	0.3360	0.0460	0.6842	290
14	0.41	168	0.0536	0.3572	0.0483	0.8116	304
15	0.26	1595	0.0529	0.3942	0.0541	0.9471	339
16	0.33	218	0.0532	0.3986	0.0544	0.8517	341
17	0.31	231	0.0539	0.3555	0.0478	0.8473	301
18	0.19	579	0.0562	0.4638	0.0599	0.9207	375
20	0.26	172	0.0520	0.3774	0.0526	0.8079	331
21	0.07	483	0.0554	0.5037	0.0660	0.7467	412
23	0.13	389	0.0563	0.5511	0.0711	0.9138	442
24	0.22	1182	0.0542	0.4260	0.0570	0.9509	308
25	0.20	829	0.0544	0.3597	0.0480	0.9299	304

observed: a small number of inherited older zircon core and rim. Inherited zircon core ages vary between ~407 Ma and 433 Ma, while rim ages range from ~301 Ma to 311 Ma. Zircon weighted mean $^{206}Pb/^{238}U$ age of the Shkhara Massif plagiogranite vein corresponds to 310.2±7 Ma (MSWD = 2.5, probability = 0.003) (Fig. 7).

Notes on the U-Th mineralization

Based on the microscopic and geochemical studies, we consider that the U and Th occur in minerals of the thorianite-uraninite series (ThO_2–UO_2). Within the crystalline structure of uraninite, the U is easily replaced by Th and, in most cases, it is represented as a solid solution of uraninite and thorianite (Anthony *et al*., 1990). Recent studies have shown that, because the uranium in silicate magma has a large ionic radius and high valence, it cannot easily enter the structure of the rock-forming minerals. This leads to the preferential existence of U in the silicate melt during the partial melting and crystal differentiation processes (*e.g*., Hazen *et al*., 2009; Cuney and Kyser, 2017). Because of the similar geochemical properties of Th and U, similar Th enrichment behavior also occurs under low-degree partial melting conditions (Kukkonen and Lauri, 2009; Chen *et al*., 2019). It is proposed that, under very low partial melting (<5%) conditions, the concentration of U in a silicate melt can reach 300 ppm **(**Mercadier *et al*., 2013).

According to Frimmel *et al*. (2014), all examples of low-temperature hydrothermal uraninite do not contain Th (U/Th > 1000), while those formed at higher temperatures (>450 °C) usually have a higher ThO_2 content (U/Th < 100). If we take into account the results of this study, the studied vein should be considered a high-temperature formation, because the U/Th ratio varies between 5.5 and 1.3 in all samples. This assumption is close to reality since, in general, the formation temperature of biotite migmatites and gneisses in the crystalline basement of the Greater Caucasus ranges from 700 °C to 750 °C (Okrostsvaridze and Tormey, 2011).

Regarding the age of radioactive mineralization, the microscopic studies show that the U-Th deposition is the youngest process that follows the rock formation. However, at this stage of research, it is impossible to determine whether it is late Variscan or younger.

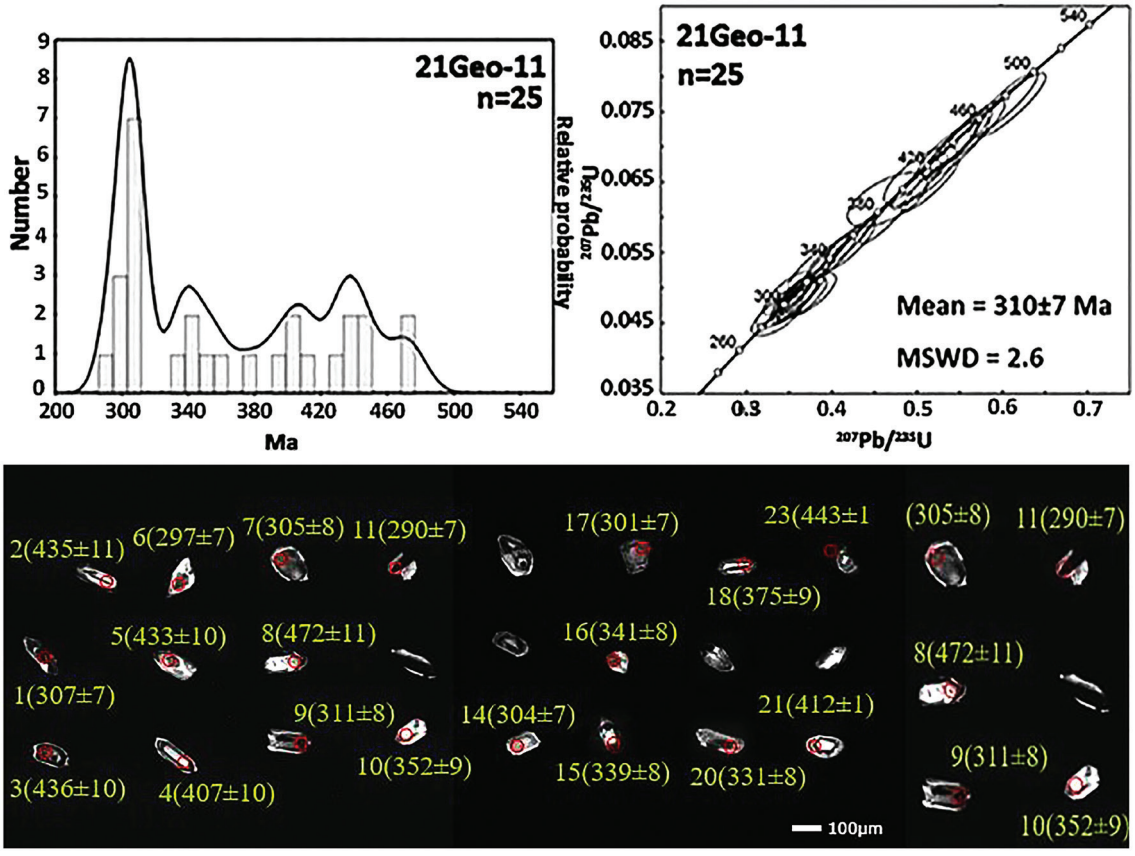

Fig. 7. $^{206}Pb/^{238}U$ age histograms (upper left), Concordia U-Pb diagram (upper right) and LA-ICP-MS cathodoluminescence images of some zircons of the Shkhara plagiogranite vein.

Due to the difficult terrain of the Shkhara Massif, the contours and scale of the studied plagiogranite vein have not been precisely determined. For the same reason, it is also impossible to trace properly such veins in the central segment of this massif. Because of this, we consider that future research of U should be carried out on the western periphery of the massif, namely in the headwaters of the River Khalde, where the terrain is easily accessible. Based on the analysis of the obtained results, the field investigation of uranium should be carried out exclusively in the late orogenic plagiogranite veins of the gneiss-migmatite complex in the Main Range Zone of the Greater Caucasus.

At the end of the discussion, we would like to mention that this discovery is the first not only in the Shkhara Massif, but also in the whole structure of the crystalline basement of the Greater Caucasus. Thus, there is still a lot of work to be done and many issues to be clarified, such as the age of U-Th mineralization, identification of their source and the scale of their distribution. We hope that, in the near future, it will be possible to answer these questions.

CONCLUSIONS

1. In the headwaters of the River Enguri, on the southern slopes of the Shkhara Massif, one of the outcropping veins of plagiogranite, ~2–3 m thick, is characterized by elevated radiation, which ranges from ~1 μSv/h to 3 μSv/h.

2. This vein is localized in the Upper–Middle Paleozoic biotite migmatites, in the contact area of the late Variscan Shkhara granitic pluton along the Greater Caucasus Main Thrust zone.

3. Petrographically, this vein is a hydrothermally altered biotite plagiogranite, in which the SiO_2 content varies from ~75% to ~85%. The U-bearing mineral is Th-rich uraninite, which is the main ore mineral for vein-type uranium deposits.

4. According to the geochemical classification diagrams, the Shkhara granitic magma belongs to the calc-alkaline series, which was generated in a volcanic arc to syn-collision geodynamic setting. Younger plagiogranite veins are possibly products of post-collision extension.

5. According to the ICP-MS analysis of samples from the vein, the Th concentration ranges from ~26 ppm to ~50 ppm, whereas U concentrations vary from ~55 ppm to ~290 ppm. It should be noted that these concentrations of U have been mined from vein-type deposits in other countries.

6. Using LA-ICP-MS analysis, $^{206}Pb/^{238}U$ age of zircons from the vein indicates an age of 310.2± 7.5 Ma that corresponds to a late Variscan orogenic activity.

7. According to the genesis, composition, magma series, geodynamic setting, tectonic localization, isotopic age and type of U mineralization, the studied vein is in full correlation with the same type of U-bearing granitic veins in different regions of the world. Based on these data, we suppose that the late Variscan hydrothermal plagiogranite veins, which are localized in the shear zones of the Shkhara Massif gneiss-migmatite complex, indicate the potential for U-bearing veins in this massif.

8. The late Variscan plagiogranite veins of the gneiss-migmatite complex of the Greater Caucasus, which are localized in the shear zones, should be a focus of detailed investigation for U-vein-type mineralization.

Acknowledgements

This research was supported by the Shota Rustaveli National Science Foundation of Georgia (SRNSFG), Grant No. FR-18-8122. We would like to give special thanks to the scientific consultant of the project, Bradley S. Van Gosen (United States Geological Survey, Denver Federal Center, Denver, USA) for selfless professional help at all stages of the project implementation. Sincere thanks to our friend Rudolf Geipel, who provided us with a radio dosimeter FAG-FH40F2, which helped discover the discussed U mineralization. We are grateful to two anonymous reviewers, whose thoughtful comments and constructive suggestions helped improve the manuscript.

REFERENCES

Andersen, T. 2002. Correction of common lead in U–Pb analyses that do not report ^{204}Pb. *Chemical Geology* 192 (1–2), 59–79, https://doi.org/10.1016/S0009-2541(02)00195-X.

Anthony, J.W., Bideaux, R.A., Bladh, K.W., Nichols, M.C. 1990. "Uraninite" Handbook of Mineralogy. *Mineralogical Society of America* 14 (2), 67–85.

Ault, T., Van Gosen, B., Krahn, S., Croff, A. 2016. Natural thorium resources and recovery: options and impacts. *Nuclear Technology* 194 (2), 136–151, https://doi.org/10.13182/NT15-83.

Ballouard, C., Poujol, M., Boulvais, P., Mercadier, J., Tartèse, R., Venneman, T., Deloule, E., Jolivet, M., Kéré, I., Cathelineau, M., Cuney, M. 2017. Magmatic and hydrothermal behavior of uranium in syntectonic leucogranites: The uranium mineralization associated with the Hercynian Guérande granite (Armorican Massif, France). *Ore Geology Reviews* 80, 309–331, https://doi.org/10.1016/j.oregeorev.2016.06.034.

Basson, I.J., Greenway, G. 2004. The Rössing Uranium Deposit: a product of late-kinematic localization of uraniferous granites in the Central Zone of the Damara Orogen, Namibia. *Journal of African Earth Sciences*, 38 (5), 413–435, https://doi.org/10.1016/j.jafrearsci.2004.04.004.

Bonnetti, C., Liu, X., Mercadier, J., Cuney, M., Deloule, E., Villeneuve, J., Liu, W. 2018. The genesis of granite-related hydrothermal uranium deposits in the Xiazhuang and Zhuguang ore fields, North Guangdong Province, SE China: Insights from mineralogical, trace elements and U-Pb isotopes signatures of the U mineralisation. *Ore Geology Reviews* 92, 588–612, https://doi.org/10.1016/j.oregeorev.2017.12.010.

Chen, Y., Hu, R., Bi, X., Luo, J. 2019. Genesis of the Guangshigou pegmatite-type uranium deposit in the North Qinling Orogenic Belt, China. *Ore Geology Reviews* 115, 103165, https://doi.org/10.1016/j.oregeorev.2019.103165.

Chi, G., Ashton, K., Deng, T., Xu, D., Li Z., Song, H., Liang, R., Kennicott, J. 2020. Comparison of granite-related uranium deposits in the Beaverlodge district (Canada) and South China – A common control of mineralization by coupled shallow and deep-seated geologic processes in an extensional setting. *Ore Geology Reviews* 117, 103119, https://doi.org/10.1016/j.oregeorev.2020.103319.

Chiu, H.-Y., Chung, S.-L., Wu, F.-Y., Liu, D., Liang, Y.-H., Lin, I.-J., Iizuka, Y., Xie, L.-W., Wang, Y., Chu, M.-F. 2009. Zircon U-Pb and Hf isotope constraints from eastern Transhimalayan batholiths on the precollisional magmatic and tectonic evolution in southern Tibet. *Tectonophysics* 477 (1–2), 3–19, https://doi.org/10.1016/j.tecto.2009.02.034.

Cuney, M. 2014. Felsic magmatism and uranium deposits. *Bulletin de la Société Géologique de France* 185 (2), 75–92, https://doi.org/10.2113/gssgfbull.185.2.75.

Cuney, P.M. Kyser, K. 2017. Geology and Geochemistry of Uranium and Thorium Deposits. *Mineralium Deposita* 52, 133–134, https://doi.org/10.1007/s00126-016-0681-9.

Descriptive Uranium Deposit and Mineral System Models. 2020. *International Atomic Energy Agency (IAEA)* ISBN: 978–92–0–109320–2, 313 pp.

Dolníček, Z., René, M., Hermannová, S., Prochaska, W. 2013. Origin of the Okrouhlá Radouň episyenite-hosted uranium deposit, Bohemian Massif, Czech Republic: fluid inclusion and stable isotope constraints. *Mineralium Deposita* 49, 409–425, https://doi.org/10.1007/s00126-013-0500-5.

Frimmel, H.E., Schedel, S., Brätz, H. 2014. Uraninite chemistry as forensic tool for provenance analysis. *Applied Geochemistry* 48, 104–121, https://doi.org/10.1016/j.apgeochem.2014.07.013.

Gamkrelidze, I.P. 1986. Geodynamic evolution of the Caucasus and adjacent areas in Alpine time. *Tectonophysics* 127 (3–4), 261–277, https://doi.org/10.1016/0040-1951(86)90064-8.

Gamkrelidze, I.P., Shengelia, D.M. 2005. *The Precambrian-Palaeozoic Regional Metamorphism, Magmatism and Geodynamics of the Caucasus*. Nauka, Moscow, 458 pp. (in Russian, with English summary).

Gamkrelidze, I.P, Shengelia, D.M., Chchindaze, G., Lee, Y.-H., Okrostsvaridze, A., Beridze, G., Vardanashvili, K. 2020. U-Pb LA-ICP-MS dating of zoned zircons from the Greater Caucasus pre-Alpine crystalline basement: Evidence for Cadomian and Variscan evolution. *Geologica Carpathica* 71 (3), 249–263, https://doi.org/10.31577/GeolCarp.71.3.4.

Groves, D.I., Bierlein F.P. 2007. Geodynamic settings of mineral deposit systems. *Journal of the Geological Society* 164 (1), 19–30, https://doi.org/10.1144/0016-76492006-065.

Harris, N., Pearce, J., Tindle, A.G. 1986. Geochemical characteristics of collision-zone magmatism. *Geological Society of London, Special Publications* 19, 67–81, https://doi.org/10.1144/GSL.SP.1986.019.01.04.

Hazen, R.M., Ewing, R.C., Sverjensky, D.A. 2009. Evolution of uranium and thorium minerals. *American Mineralogist* 94 (10), 1293–1311, https://doi.org/10.2138/am.2009.3208.

Hofmann, B., Eikenberg, J. 1991. The Krunkelbach uranium deposit, Schwarzwald, Germany; correlation of radiometric ages (U-Pb, U-Xe-Kr, K-Ar, 230 Th- 234 U). *Economic Geology* 86 (5), 1031–1049, https://doi.org/10.2113/gsecongeo.86.5.1031.

International Commission on Radiological Protection. 2007 Recommendations of the International Commission on Radiological Protection. *ICRP Publication* 103, 171, https://doi.org/10.1016/j.icrp.2007.10.003.

Irvine, T.N., Baragar, W.R. 1971. A guide to the chemical classification of the common volcanic rocks. *Canadian Journal of Earth Sciences* 8 (5), 523–548, https://doi.org/10.1139/e71-055.

Jackson, S., Pearson, N., Griffin, W., Belousova, E. 2004. The application of laser ablation-inductively coupled plasma-mass spectrometry to in situ U-Pb zircon geochronology. *Chemical Geology* 211 (1–2), 47–69, https://doi.org/10.1016/j.chemgeo.2004.06.017.

Kukkonen, I., Lauri, L. 2009. Modelling the thermal evolution of a collisional Precambrian orogen: High heat production migmatitic granites of southern Finland. *Precambrian Research* 168 (3–4), 233–246, https://doi.org/10.1016/j.precamres.2008.10.004.

López-Moro, F.J., Romer, L.R., Rhede, D., Fernandez, A., Timón-Sánchez, S.M., Moro, M.C. 2019. Early uranium mobilization in late Variscan strike-slip shear zones affecting leucogranites of central western Spain. *Journal of Iberian Geology* 45, 223–243, https://doi.org/10.1007/s41513-018-0091-1.

Ludwig, K.R. 2003. User's manual for Isoplot 3.00: a geochronological toolkit for Microsoft Excel. *Berkeley Geochronology Center, Special Publication* 4, 74 pp.

Mercadier, J., Annesley, I.R., McKechnie, C.L., Bogdan, T.S., Creighton, S. 2013. Magmatic and metamorphic uraninite mineralization in the western margin of the Trans-Hudson Orogen (Saskatchewan, Canada): A uranium source for unconformity-related uranium deposits?. *Economic Geology* 108 (5), 1037–1065, https://doi.org/10.2113/econgeo.108.5.1037.

Middlemost, E.A.K. 1994. Naming materials in the magma/igneous rock system. *Earth-Science Reviews* 37 (3–4), 215–224, https://doi.org/10.1016/0012-8252(94)90029-9.

Odikadze, G.L. 1971. Uranium and thorium in the granitoids of the Greater Caucasus and the Dzirula Massif. *Proceedings of the Caucasus Institute of Mineral Resources*, 165–175 (in Russian).

Okrostsvaridze, A. 1995. *Petrology of Hercynian plutonic series of the Greater Caucasus*. PhD thesis, Tbilisi, Georgia, 315 pp. (in Georgian).

Okrostsvaridze, A. 2007. *Hercynian Granitoid Magmatism of the Greater Caucasus.* Intelect, Tbilisi, 223 pp. (in Russian, with English summary).

Okrostsvaridze, A., Tormey, D. 2011. Evolution of the Variscan orogenic plutonic magmatism: The Greater Caucasus. *Journal of Nepal Geological Society* 43 (Special Issue), 45–52, https://doi.org/10.3126/jngs.v43i0.24514.

Okrostsvaridze, A., Tormey, D. 2013. Phanerozoic continental crust evolution of the Inner Caucasian Microplate, The Dzirula Massif. *Episodes* 36 (1), 31–38, https://doi.org/10.18814/epiiugs/2013/v36i1/005.

Okrostsvaridze, A., Bluashvili, D., Gagnidze, N. 2014. Field investigation of the mythical "Gold Sands" of the ancient Colchis Kingdom and modern discussion on Argonauts' expedition. *Episodes* 37 (2), 122–128, https://doi.org/10.18814/epiiugs/2014/v37i2/007.

Okrostsvaridze, A., Gagnidze, N., Boichenko, G. 2016. Geological framework and mineral occurrences in the Georgia segment of the Eastern Greater Caucasus. *Episodes* 39 (3), 500–508, https://doi.org/10.18814/epiiugs/2016/v39i3/99770.

Okrostsvaridze, A., Gogoladze, S. 2017. Thorium Resources and their Energy Potential in Georgian Republic, the Caucasus. *Energy Prosedia* 125, 291–299, https://doi.org/10.1016/j.egypro.2017.08.185.

Pearce, J.A. 1996. Source and setting of granitic rocks. *Episodes* 19 (4), 120–125, https://doi.org/10.18814/epiiugs/1996/v19i4/005.

Ridley, J. 2013. *Ore Deposit Geology*. Cambridge University Press, Cambridge, 398 pp., https://doi.org/10.1017/CBO9781139135528.

Richards, J.P. 2015. Tectonic, magmatic, and metallogenic evolution of the Tethyan orogen: from subduction to collision. *Ore Geology Review* 70, 323–345, https://doi.org/10.1016/j.oregeorev.2014.11.009.

René, M. 2012. Uranium hydrothermal deposits. *In*: Vasiliev, A.Y., Sidorov, M. (Eds), *Uranium: Characteristics, Occurrence and Human Exposure*. Nova Science Publishers Incorporated, 211–244.

Şengör, A.M.C., Yılmaz, Y. 1981. Tethyan evolution of Turkey: a plate tectonic approach. *Tectonophysics* 75 (3–4), 181–241, https://doi.org/10.1016/0040-1951(81)90275-4.

Sláma, J., Košler, J., Condon, D.J., Crowley, J.L., Gerdes, A., Hanchar, J.M., Horstwood, M.S.A., Morris, G.A., Nasdala, L., Norberg, N., Schaltegger, U., Schoene, B., Tubrett, M.N., Whitehouse, M.J. 2008. Plešovice zircon – a new natural reference material for U-Pb and Hf isotopic microanalysis. *Chemical Geology* 249 (1–2), 1–35, https://doi.org/10.1016/j.chemgeo.2007.11.005.

Somin, M.L. 2011. Pre-Jurassic basement of the Greater Caucasus: Brief overview. *Turkish Journal of Earth Sciences* 20, 545–610, https://doi.org/10.3906/yer-1008-6.

Stampfli, G.M., Borel, G.D. 2004. A plate tectonic model for the Paleozoic and Mesozoic constrained by dynamic plate boundaries and restored synthetic oceanic isochrones. *Earth and Planetary Science Letters* 196 (1–2), 17–33, https://doi.org/10.1016/S0012-821X(01)00588-X.

Tulsidas, H., van Gosen, B.S., Griffiths, C., Barrett, A., Lopez, L., Villas-Bôas, R., Shengxiang, L., Ross, J., Bankes, P., Hilton, J., Heiberg, S., MacDonald, D., Hanly, A. 2015. Guidelines for application of the United Nations framework classification for resources (UNFC) to uranium and thorium resources. *Report of the United Nations Economic Commission for Europe*, 71 pp., https://doi.org/10.13140/RG.2.1.1805.0328.

van Gosen, B.S., Gillerman, V.S., Armbrustmacher, T.J. 2009. Thorium deposits of the United States – Energy resources for the future?. *U.S. Geological Survey Circular* 1336, 21 pp., https://doi.org/10.3133/cir1336.

Zhang, C., Cai, Y., Xu, H., Dong, Q., Liu, J., Hao, R. 2017. Mechanism of mineralization in the Changjiang uranium ore field, South China: Evidence from fluid inclusions, hydrothermal alteration, and H-O isotopes. *Ore Geology Reviews* 86, 225–253, https://doi.org/10.1016/j.oregeorev.2017.01.013.

Zheng, Y., Mao, J., Chen, Y., Sun, W., Pei, N., Yang, X. 2019. Hydrothermal ore deposits in collisional orogens. *Science Bulletin* 64 (3), 205–212, https://doi.org/10.1016/j.scib.2019.01.007.